JACS
JOURNAL OF THE AMERICAN CHEMICAL SOCIETY

COMMUNICATION

pubs.acs.org/JACS

Plasmonic Imaging of Human Oral Cancer Cell Communities during Programmed Cell Death by Nuclear-Targeting Silver Nanoparticles

Lauren A. Austin, Bin Kang,[‡] Chun-Wan Yen, and Mostafa A. El-Sayed*

Laser Dynamics Laboratory, School of Chemistry and Biochemistry, Georgia Institute of Technology, Atlanta, Georgia 30332-0400, United States

Supporting Information

ABSTRACT: Plasmonic nanoparticles (NPs) have become a useful platform in medicine for potential uses in disease diagnosis and treatment. Recently, it has been reported that plasmonic NPs conjugated to nuclear-targeting peptides cause DNA damage and apoptotic populations in cancer cells. In the present work, we utilized the plasmonic scattering property and the ability of nuclear-targeted silver nanoparticles (NLS/RGD-AgNPs) to induce programmed cell death in order to image in real-time the behavior of human oral squamous carcinoma (HSC-3) cell communities during and after the induction of apoptosis. Plasmonic live-cell imaging revealed that HSC-3 cells behave as nonprofessional phagocytes. The induction of apoptosis in some cells led to attraction of and their subsequent engulfment by neighboring cells. Attraction to apoptotic cells resulted in clustering of the cellular community. Live-cell imaging also revealed that, as the initial concentration of NLS/RGD-AgNPs increases, the rate of self-killing increases and the degree of attraction and clustering decreases. These results are discussed in terms of the proposed mechanism of cells undergoing programmed cell death.

Plasmonic nanoparticles (NPs) have received considerable attention in the biological and biomedical community due to their potential use in diagnostic and therapeutic applications.[1,2] Their ability to scatter light in the visible and near-infrared regions has been used in biological imaging and cancer diagnostic applications.[3,4] Additionally, their nanoscale size allows them to enter the cell and target different organelles, such as the nucleus and mitochondria.[5−8] As their popularity in medical and everyday applications has increased, several studies have been conducted to investigate their cytotoxic effects on mammalian cells.[9−17] Studies examining the toxicity of gold nanoparticles (AuNPs), with diameter >1.4 nm, have shown minimal cell death with incubation periods of up to 3 days.[16,17] Conversely, several reports have shown that mammalian cells experience increased programmable cell death (apoptosis) after incubation with conjugated and unconjugated silver nanoparticles (AgNPs).[11,14,15] The suggested cause for apoptosis in AgNP-treated cells is the generation of reactive oxygen species (ROS), which is known to cause irreversible DNA damage.[18−20]

Apoptosis is a highly controlled cellular process and plays an important role in regulating tissue homeostasis and controlling physiological growth.[21,22] Induction of apoptosis can occur from a variety of stimulating agents, which are generally grouped into two categories: extrinsic or intrinsic.[23,24] Extrinsic stimuli are those that cause cell death signaling from death receptor ligation. After ligation, cytoplasmic signaling pathways are activated, and apoptosis is triggered. Intrinsic apoptosis is usually induced through generation of metabolic or genotoxic stress. One of the most notable intrinsic pathways, the p53 pathway, is activated from DNA damage that results from oxidative stress.[23] It is thought that AgNPs induce apoptosis by acting as intrinsic stimuli due to their ability to generate ROS and cause DNA double-strand breaks (DSBs).[11,25] In the present work, we exploit the plasmonic light-scattering properties and the cellular apoptotic induction of AgNPs to investigate the behavior of human oral squamous carcinoma (HSC-3) cellular communities undergoing apoptosis.

Plasmonic AgNPs were synthesized using previously reported methods.[26,27] The synthesized 35 nm NPs (Figure 1) were then conjugated with mPEG-SH 5000 to achieve a maximum surface coverage of 10%. The low poly(ethylene glycol) (PEG) surface coverage was chosen to maximize peptide conjugation to the AgNPs.[28] Pegylation of the NPs aids in stabilizing the particles in cell culture media and reduces protein absorption on the particles' surface.[29] The remaining surface of the NPs was conjugated to nuclear localizing signal (NLS) and cancer cell penetrating (RGD) peptides.

The cells used in this study, HSC-3, have been shown to express $\alpha_v\beta_6$ integrins on their surfaces.[30] The RGD peptides conjugated to the surface of the AgNPs assist in uptake of the particles by aiding in receptor-mediated endocytosis through their interaction with the $\alpha_v\beta_6$ surface integrins.[31] After the particles enter the cytoplasm, they become localized at the nucleus due to the interaction between the NLS peptide on the particles' surface and importins α and β, karyopherins that are associated with the nuclear pore complex (NPC).[32,33] In recent work, localization of plasmonic (Au and Ag) NPs at the nucleus of HSC-3 cells was found to result in DNA DSBs and apoptotic (or DNA-deficient) populations.[34,35]

To ensure NLS/RGD-AgNPs were the most efficient at inducing cell death, we conducted in vitro cytotoxicity (XTT) assays on both pegylated and peptide-conjugated AgNPs. HSC-3 cells were incubated with 0.1 nM conjugated AgNPs for 24 h. As shown in Figure 2, NLS/RGD-AgNPs (nuclear-targeting) showed the highest cytotoxicity, with ∼54% cell viability, while RGD- and PEG-conjugated particles showed minimal toxicity, with viabilities >91%. These results demonstrate the necessity of NLS−peptide conjugation to induce cell death, as RGD- and PEG-conjugated

Received: August 17, 2011
Published: October 07, 2011

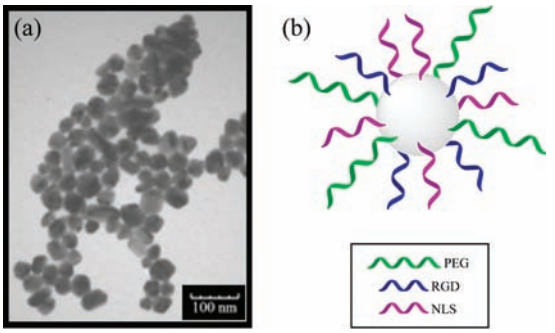

Figure 1. (a) TEM micrograph of the synthesized citrate-capped AgNPs (~35 nm). (b) Illustration of AgNPs conjugated to PEG and cancer-targeting (RGD) and nuclear-targeting (NLS) peptides.

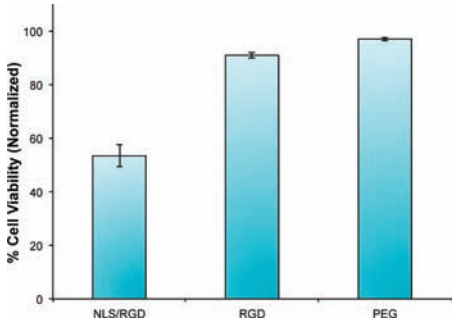

Figure 2. Viability of HSC-3 cells incubated with 0.1 nM conjugated AgNPs after 24 h. Overall NLS/RGD-AgNPs showed greater cytotoxicity (~52% cell viability) than RGD- and PEG-conjugated AgNPs (~90% viability). This supports the proposal that NLS is needed to localize AgNPs at the nucleus and cause cell death.

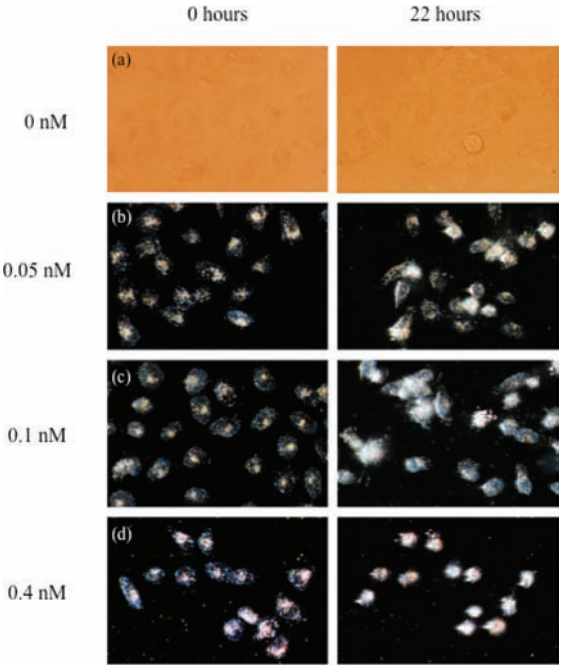

Figure 3. Still images taken at 0 and 22 h of HSC-3 cells incubated with (a) 0, (b) 0.05, (c) 0.1, and (d) 0.4 nM nuclear-targeting AgNPs. Cells treated with 0 nM AgNPs do not show plasmonic light scattering. Images of cells treated with NLS/RGD-AgNPs show that (1) scattering from the AgNPs is heavily localized at the nucleus, (2) cellular clustering increases as the AgNP concentration increases from 0.05 to 0.1 nM, and (3) the degree of cellular clustering decreases when cells are treated with 0.4 nM AgNPs. The observed decrease in clustering could be attributed to the increased rate of the observed cell death. The high AgNP density at the cell nucleus, as indicated by the strong scattering (d), is the reason for the rapid cell death (see text) for most cells and could impair the ability of these cells to produce or detect intercellular apoptotic signals.

AgNPs did not show significant toxicity. Due to their relatively high toxicity and their ability to cause DNA damage through the generation of ROS as seen in our previous work,[35] NLS/RGD-AgNPs were chosen for this study, as they are the most effective in inducing apoptosis.

In this work, plasmonic live-cell imaging[36] was used to investigate the behavior of cancer cell communities after incubation with varying concentrations (0, 0.05, 0.1, and 0.4 nM) of nuclear-targeting NLS/RGD-AgNPs (see Supporting Information movies 1−4). Cells were incubated for 24 h with nuclear-targeting particles before imaging to allow for successful uptake and disturbance of cellular functions. Representative live-cell images at 0 and 22 h for each tested concentration are shown in Figure 3. Untreated cancer cells were able to divide successfully and maintained their original distribution between neighboring cells (Figure 3a and SI movie 1). However, incubation with NLS/RGD-AgNPs stopped cell division and ultimately caused cell death. Apoptosis was the suggested form of cell death due to visible cell shrinkage, a morphological characteristic of apoptotic cells,[37] and our results from previous flow cytometry studies,[35] which showed an increase in the sub-G1 (or apoptotic/DNA deficient) population in HSC-3 cells after incubation with NLS/RGD-AgNPs. Interestingly, the video clearly shows that when cells are subjected to initial loadings of 0.05 and 0.1 nM AgNPs and one cell dies (cell becomes still and white in color due to the loss of focus as they become detached), the live neighboring cells, which also contain NLS/RGD-AgNPs, move within close proximity to the dying cell and proceed to engulf the apoptotic cell. The attraction of neighboring cells caused a reduction in the initial random spatial distribution of the cancer cell community and resulted in cellular clustering (Figure 3b,c and SI movies 2 and 3). At higher initial loading concentrations (0.4 nM) of AgNPs (Figure 3d and SI movie 4), the clustering is greatly reduced or stopped.

The cellular clustering seen throughout the cancer community (Figure 3b,c and SI movies 2 and 3) is thought to be a result of apoptotic signaling. As stated previously, apoptosis is necessary for maintaining homeostasis and regulating tissue growth.[21,22] However, dying cells need to be identified and removed to avoid the loss of membrane integrity and the potential release of cytotoxins. Traditionally, professional phagocytes, such as macrophages and immature dendritic cells, facilitate apoptotic cell removal. For cell removal to occur, apoptotic cells display "eat me" signals on their cell surface to attract professional phagocytes and aid in their subsequent engulfment.[38] The most notable signals include annexin I (AnxI) and phosphatidylserine (PS), which are translocated to the outer cellular membrane. Additionally, professional phagocytes contain PS and vibronectin ($\alpha_v\beta_3$) receptors that assist in "eat me" signal recognition and uptake of apoptotic cells.[39]

Although professional phagocytes are usually involved in the removal of apoptotic cells, other cell types, such as epithelial cells and fibroblasts, are known to perform phagocytosis and are collectively termed nonprofessional phagocytes.[40] Since our cell line

dx.doi.org/10.1021/ja207807t |J. Am. Chem. Soc. 2011, 133, 17594–17597

is classified as an epithelial cell line and has been shown to express $\alpha_v\beta_3$ receptors and AnxI, it is possible that HSC-3 cells also act as nonprofessional phagocytes.[30] As seen from our video imaging (Figure 3b,c and SI movies 2 and 3), once one cell undergoes apoptosis, the neighboring cells move and recognize the dying cell. Characteristic palpitating and cohesive movements of the live and dying cells indicated successful apoptotic identification. The observed clustering was the consequence of the identification of the dying cell by several neighboring cells which have less AgNP DNA damage and are still viable. After the apoptotic cell had been identified, the live neighboring cells proceeded to engulf the dying cell. Engulfment was suggested by the merger of the live and dying cells, which caused the live cell to become unfocused and bright white, like the apoptotic cell. Unlike professional phagocytes, nonprofessional phagocytes require longer periods of time to ingest an apoptotic cell.[41] This characteristic is also seen in our video imaging, as recognition of the dying cell occurs rather quickly, but engulfment requires several hours. The extended time for ingestion is most likely due to the apoptotic cell needing to undergo further changes to signal to nonprofessional phagocytes for engulfment.[41]

In addition to the observed cellular clustering around the apoptotic cell, there also appears to be an increased localization of cell deaths. It has been reported by several groups that cellular clusters collectively undergo apoptosis after the apoptotic induction of a single cell within the cluster.[25] Thubagere et al.[25] recently showed that Caco-2 cells (heterogeneous human epithelial colorectal adenocarcinoma cells) underwent cellular apoptotic clustering after incubation with polystyrene NPs. They attributed the propagation of apoptosis throughout the cellular community to the production of hydrogen peroxide, which they proposed was released into the extracellular environment. Nano-size metal oxide materials, especially Ag_2O, which is formed from oxidation of the AgNPs' surfaces, are known to generate ROS including hydrogen peroxide.[19] Although ROS are a natural byproduct of cellular metabolism (i.e., oxidative phosphorylation) during the production of ATP, increased concentrations of these species, especially hydrogen peroxide, causes oxidative damage that results in DNA damage and apoptosis. As indicated from our previous papers, DNA damage was indeed found to occur in HSC-3 cells treated with nuclear-targeting NPs and was attributed to the generation of ROS.[34,35] In this study, it is suggested that ROS generated from the NLS/RGD-AgNPs are released into the extracellular environment and cause an increase in the local concentration of ROS near the apoptotic cell. The increased local concentration resulted in the permeation of ROS through the membranes of neighboring cells. Additionally, a successive heightening of apoptotic signaling within the neighboring cells, as these cells also contain NLS/RGD-AgNPs, is thought to have occurred, which led to the observed localization of cell death near the primary apoptotic cell.

As shown in Figure 3d and SI movie 4, when the loading concentration of NLS/RGD-AgNPs reached 0.4 nM, cellular clustering greatly diminished or stopped. This observation might suggest that, at this high concentration of AgNPs, most of the cells die at rapid and comparable rates. Using SI movie 4, it can be estimated that the initial death rate of cells at initial AgNP loading concentrations of 0.05, 0.1, and 0.4 nM are 0.05, 0.1, and 0.25 h^{-1}, respectively. The increased death rate of the 0.4 nM sample is expected to impair the cells' ability to sense or display intercellular apoptotic signals as well as hinder their movement and clustering. Since the nuclear-targeting AgNPs are thought to be the initial cause of apoptosis, one may conclude that intracellular and intercellular apoptotic signaling (i.e., PS and AnxI) are competitive processes. The quicker intracellular apoptotic signaling is induced in cells of a community, the less likely it is that intercellular communication and clustering of cells will occur.

In conclusion, we used plasmonic live-cell imaging to study the resulting behavior of cancer cell communities when apoptotic induction occurs in one or several cells within the community. Our imaging revealed cellular attraction, clustering, and bystander killing after incubation with apoptosis-inducing AgNPs at low concentrations. It is suggested that cells neighboring an apoptotic cell act as nonprofessional phagocytes and are attracted to and engulf the dying cell through "eat me" signals such as PS and AnxI, which are displayed on the apoptotic cell's surface. The resulting cellular clustering allowed ROS generated from the NLS/RGD-AgNPs and released from the apoptotic cell to permeate the neighboring cells' membranes and cause a localization of cell death. At high AgNP concentrations (and increased rate of programmed cell death), the degree of attraction and clustering is diminished. This is presumably due to simultaneous death of most cells that impairs their ability to move and cluster.

It is interesting to point out that the plasmonic live-cell imaging and nuclear-targeting AgNPs used in this study had the ability to visually investigate intercellular responses to external stimuli in a cellular community without the need to use fluorescent dyes and expensive microscopic equipment.

■ ASSOCIATED CONTENT

Supporting Information. Experimental details, UV−vis spectra, and plasmonic live-cell imaging movies. This material is available free of charge via the Internet at http://pubs.acs.org.

■ AUTHOR INFORMATION

Corresponding Author
melsayed@gatech.edu

Present Addresses
[‡]College of Material Science and Technology, Nanjing University of Aeronautics and Astronautics, Nanjing 210016, P.R. China

■ ACKNOWLEDGMENT

M.A.E. acknowledges the Julius Brown Chair Funding (3306559GT) and the NIH-NCI (U01CA151802-01). L.A.A. thanks the GT GAANN fellowship (3306FT8), and B.K. thanks the China Scholar Council (2008683010) and the Doctor Innovation Funds of China NUAA (BCXJ08-09). The authors thank Brian Snyder for taking TEM micrographs of the synthesized AgNPs.

■ REFERENCES

(1) Huang, X.; Jain, P. K.; El-Sayed, I. H.; El-Sayed, M. A. *Nanomedicine* **2007**, *2*, 681.
(2) Dreaden, E. C.; Mackey, M. A.; Huang, X.; El-Sayed, M. A. *Chem. Soc. Rev.* **2011**, *40*, 3391.
(3) Huang, X.; El-Sayed, I. H.; Qian, W.; El-Sayed, M. A. *J. Am. Chem. Soc.* **2006**, *128*, 2115.
(4) Liu, X.; Dai, Q.; Austin, L.; Coutts, J.; Knowles, G.; Zou, J.; Chen, H.; Huo, Q. *J. Am. Chem. Soc.* **2008**, *130*, 2780.
(5) Tkachenko, A. G.; Xie, H.; Coleman, D.; Glomm, W.; Ryan, J.; Anderson, M. F.; Franzen, S.; Feldheim, D. L. *J. Am. Chem. Soc.* **2003**, *125*, 4700.

(6) Oyelere, A. K.; Chen, P. C.; Huang, X.; El-Sayed, I. H.; El-Sayed, M. A. *Bioconjugate Chem.* **2007**, *18*, 1490.
(7) Murphy, M. P. *Trends Biotechnol.* **1997**, *15*, 326.
(8) Murphy, M. P.; Smith, R. A. *J. Adv. Drug Delivery Rev* **2000**, *41*, 235.
(9) AshaRani, P. V.; Low Kah Mun, G.; Hande, M. P.; Valiyaveettil, S. *ACS Nano* **2008**, *3*, 279.
(10) Braydich-Stolle, L.; Hussain, S.; Schlager, J. J.; Hofmann, M.-C. *Toxicol. Sci.* **2005**, *88*, 412.
(11) Foldbjerg, R.; Olesen, P.; Hougaard, M.; Dang, D. A.; Hoffmann, H. J.; Autrup, H. *Toxicol. Lett.* **2009**, *190*, 156.
(12) Hussain, S. M.; Hess, K. L.; Gearhart, J. M.; Geiss, K. T.; Schlager, J. J. *Toxicol. in Vitro* **2005**, *19*, 975.
(13) Kawata, K.; Osawa, M.; Okabe, S. *Environ. Sci. Technol.* **2009**, *43*, 6046.
(14) Lee, Y.; Kim, D.; Oh, J.; Yoon, S.; Choi, M.; Lee, S.; Kim, J.; Lee, K.; Song, C.-W. *Arch. Toxicol.* **2011**, 1.
(15) Park, E.-J.; Yi, J.; Kim, Y.; Choi, K.; Park, K. *Toxicol. in Vitro* **2010**, *24*, 872.
(16) Murphy, C. J.; Gole, A. M.; Stone, J. W.; Sisco, P. N.; Alkilany, A. M.; Goldsmith, E. C.; Baxter, S. C. *Acc. Chem. Res.* **2008**, *41*, 1721.
(17) Pan, Y.; Neuss, S.; Leifert, A.; Fischler, M.; Wen, F.; Simon, U.; Schmid, G.; Brandau, W.; Jahnen-Dechent, W. *Small* **2007**, *3*, 1941.
(18) Moustafa, M. H.; Sharma, R. K.; Thornton, J.; Mascha, E.; Abdel-Hafez, M. A.; Thomas, A. J.; Agarwal, A. *Hum. Reprod.* **2004**, *19*, 129.
(19) Azzam, E. I.; de Toledo, S. M.; Little, J. B. *Oncogene* **2003**, *22*, 7050.
(20) Simon, H. U.; Haj-Yehia, A.; Levi-Schaffer, F. *Apoptosis* **2000**, *5*, 415.
(21) Alenzi, F. *Br. J. Biomed. Sci.* **2004**, *61*, 99.
(22) Jacobson, M. D.; Weil, M.; Raff, M. C. *Cell* **1997**, *88*, 347.
(23) Wang, J. Y. J. *Cell Res.* **2005**, *15*, 43.
(24) Fulda, S.; Debatin, K. M. *Oncogene* **2006**, *25*, 4798.
(25) Thubagere, A.; Reinhard, B. M. *ACS Nano* **2010**, *4*, 3611.
(26) Freund, P. L.; Spiro, M. *J. Phys. Chem.* **1985**, *89*, 1074.
(27) Kimling, J.; Maier, M.; Okenve, B.; Kotaidis, V.; Ballot, H.; Plech, A. *J. Phys. Chem. B* **2006**, *110*, 15700.
(28) Huang, X.; Kang, B.; Qian, W.; Mackey, M. A.; Chen, P. C.; Oyelere, A. K.; El-Sayed, I. H.; El-Sayed, M. A. *J. Biomed. Opt.* **2010**, *15*, 058002.
(29) Wuelfing, W. P.; Gross, S. M.; Miles, D. T.; Murray, R. W. *J. Am. Chem. Soc.* **1998**, *120*, 12696.
(30) Xue, H.; Atakilit, A.; Zhu, W.; Li, X.; Ramos, D. M.; Pytela, R. *Biochem. Biophys. Res. Commun.* **2001**, *288*, 610.
(31) Chen, X.; Plasencia, C.; Hou, Y.; Neamati, N. *J. Med. Chem.* **2005**, *48*, 1098.
(32) Panyam, J.; Labhasestwar, V. *Curr. Drug Delivery* **2004**, *1*, 235.
(33) Dingwall, C.; Laskey, R. A. *Trends Biochem. Sci.* **1991**, *16*, 478.
(34) Kang, B.; Mackey, M. A.; El-Sayed, M. A. *J. Am. Chem. Soc.* **2010**, *132*, 1517.
(35) Austin, L. A.; Kang, B.; Yen, C.; El-Sayed, M. A. *Bioconjugate Chem.* **2011**submitted.
(36) Qian, W.; Huang, X.; Kang, B.; El-Sayed, M. A. *J. Biomed. Opt.* **2010**, *15*, 046025.
(37) Gerschenson, L.; Rotello, R. *FASEB* **1992**, *6*, 2450.
(38) Grimsley, C.; Ravichandran, K. S. *Trends Cell Biol.* **2003**, *13*, 648.
(39) Hisatomi, T.; Sakamoto, T.; Sonoda, K.-h.; Tsutsumi, C.; Qiao, H.; Enaida, H.; Yamanaka, I.; Kubota, T.; Ishibashi, T.; Kura, S.; Susin, S. A.; Kroemer, G. *Am. J. Pathol.* **2003**, *162*, 1869.
(40) Rabinovitch, M. *Trends Cell Biol.* **1995**, *5*, 85.
(41) Parnaik, R.; Raff, M. C.; Scholes, J. *Curr. Biol.* **2000**, *10*, 857.